International Journal of Minerals, Metallurgy and Materials
Volume 22, Number 8, August 2015, Page 788
DOI: 10.1007/s12613-015-1135-6

New pyrometallurgical process of EAF dust treatment with CaO addition

Romchat Chairaksa-Fujimoto[1)], *Yosuke Inoue*[2)], *Naoyoshi Umeda*[3)], *Satoshi Itoh*[1)], *and Tetsuya Nagasaka*[1)]

1) Department of Metallurgy, Graduate School of Engineering, Tohoku University, 6–6–02, Aramaki-Aza-Aoba, Aoba-ku, Sendai 980–8579, Japan
2) Toho Titanium Co., Ltd., 3–5–5, Chigasaki, Chigasaki City, Kanagawa 253–8510, Japan
3) Honda Motor Co., Ltd., 1–13–1, Aoihigashi Naka-ku Hamamatsu-City Shizuoka 433–8501, Japan
(Received: 5 January 2015; revised: 16 March 2015; accepted: 17 March 2015)

Abstract: The non-carbothermic zinc pyrometallurgical processing of electric arc furnace (EAF) dust was investigated on a laboratory scale. The main objective of this process was to convert highly stable zinc ferrite ($ZnFe_2O_4$), which accounts for more than half of total zinc in the EAF dust, into ZnO and $Ca_2Fe_2O_5$ by CaO addition. The EAF dust was mixed with CaO powder in various ratios, pressed into pellets, and heated in a muffle furnace in air at temperatures ranging from 700 to 1100°C for a predetermined holding time. All $ZnFe_2O_4$ was transformed into ZnO and $Ca_2Fe_2O_5$ at a minimum temperature of 900°C within 1 h when sufficient CaO to achieve a Ca/Fe molar ratio of 1.1 was added. However, at higher temperatures, excess CaO beyond the stoichiometric ratio was required because it was consumed by reactions leading to the formation of compounds other than $ZnFe_2O_4$. The evaporation of halides and heavy metals in the EAF dust was also studied. These components could be preferentially volatilized into the gas phase at 1100°C when CaO was added.

Keywords: electric arc furnace dust; pyrometallurgy; zinc oxide; zinc ferrite; calcium oxide

1. Introduction

Zinc has been used mainly in the process of galvanizing steel and its consumption is increasing annually [1]. After five to ten years of use, end-of-life galvanized steel products are collected as scrap and remelted in electric arc furnaces (EAFs) for steel recycling. During the process of melting scrap in EAFs, most of the zinc is evaporated because of its relatively low boiling point (907°C) and collected in a bag filter as EAF dust; the average zinc content of this dust is approximately 20wt% [2–4]. The composition of EAF dust depends on the EAF operating conditions, such as the characteristics of the scrap charged into the EAF, the electric power supplied to the EAF, the operating period, the specification of the steel produced, etc. [5]. Given an average yield of EAF dust of 15 to 25 kg for every metric ton of steel produced [6], the amount of zinc that can possibly be recovered from EAF dust is approximately 1.4 million tons worldwide per annum [7]. However, EAF dust has been classified as a hazardous waste by various government regulatory agencies according to the toxicity characteristic leaching procedure (TCLP) of lead, cadmium, and chromium [4–5,8–13].

Two main approaches for treating the dust have been developed: stabilization or vitrification prior to landfilling and metals recovery for recycling [5,13–14]. Zinc has been recognized as one of the elements whose supply in nature is possibly limited [15]. Hence, zinc recovery from EAF dust has become an important issue for zinc resources conservation because no other essential zinc recycling path from the end-of-life zinc products exists, as schematically shown in Fig. 1 [16]. Various pyrometallurgical and hydrometallurgical techniques have been developed for the intermediate treatment of EAF dust; those that have worked on a commercial scale are generally high-temperature zinc oxide recovery processes—specifically, the Waelz rotary kiln process and rotary hearth furnace technology [12,17–18]. Both of these processes are based on the reduction and volatilization of zinc from EAF dust by carbothermic reduction; however, they produce ZnO, which requires further proc-

Corresponding author: Romchat Chairaksa-Fujimoto E-mail: chairaksaromchat@material.tohoku.ac.jp
© University of Science and Technology Beijing and Springer-Verlag Berlin Heidelberg 2015

essing, rather than metallic zinc [5,7,12,14,19–20]. In addition, the by-product solid residue (clinker) containing iron from the Waelz process, which was previously used as cement or road construction material, can no longer be reused in this manner because of new environmental regulations [21–23].

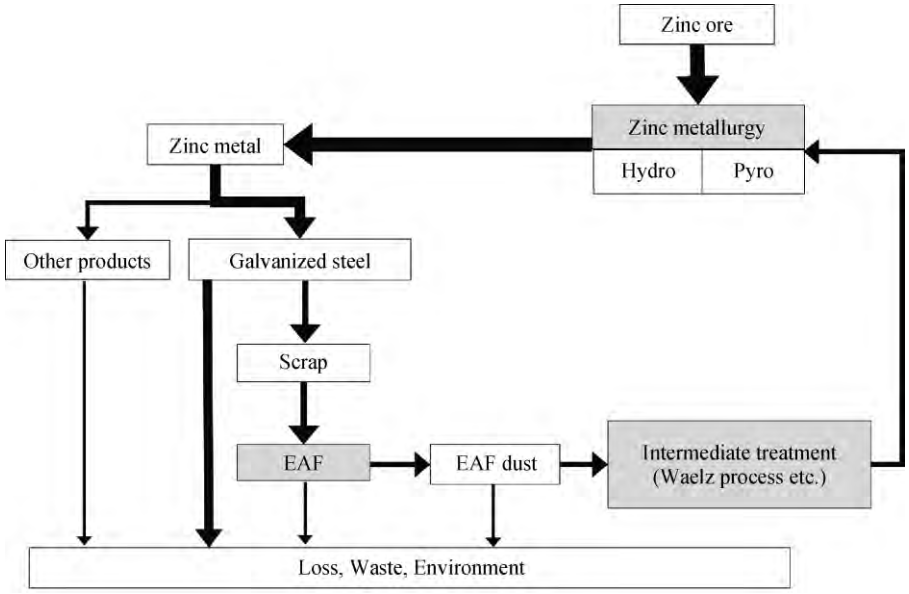

Fig. 1. Schematic of the zinc cycle via EAF dust.

The difficulties associated with the intermediate treatment of EAF dust are as follows: (1) the major species of zinc in the dust is zinc ferrite ($ZnFe_2O_4$), which is difficult to leach or reduce [14,19]; and (2) the dust contains relatively high concentrations of halogens (chlorine and fluorine) and heavy metals (lead and, in some cases, cadmium). For the conversion of $ZnFe_2O_4$ to ZnO with lower energy input, we have proposed a new process for dust pretreatment that we refer to as the "CaO addition process" [21–24]. $ZnFe_2O_4$ in the dust can react with CaO to form ZnO and $Ca_2Fe_2O_5$ via the following reaction:

$$ZnFe_2O_4(s) + 2CaO(s) = ZnO(s) + Ca_2Fe_2O_5(s) \quad (1)$$

$$\Delta G_1^{\ominus} = -32114 + 11.329T + 4.201\times10^{-3}T^2 - 5.46\times10^5/T - 3.373T\ln T \text{, J/mol} \quad (2)$$

$$\Delta H_1^{\ominus} = -32114 + 3.373T - 4.201\times10^{-3}T^2 - 10.91\times10^5/T \text{, J/mol} \quad (3)$$

As presented in Fig. 2, the values of both the free energy and the enthalpy changes of this reaction are negative at elevated temperatures, and the exothermic nature of this

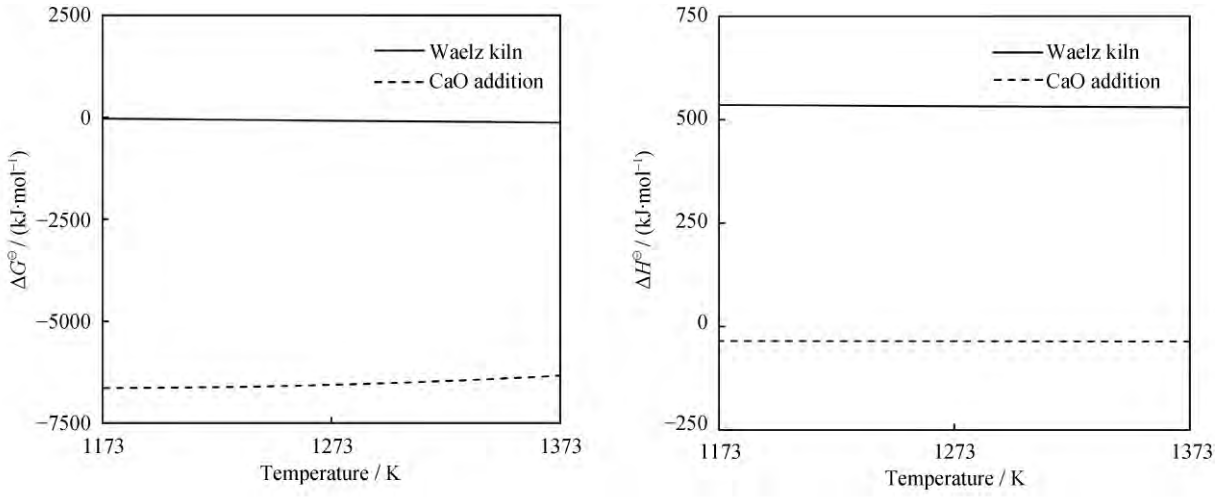

Fig. 2. Comparison of free energy and the enthalpy changes between the Waelz process and the CaO addition process at 900 to 1100°C.

reaction is a benefit of the CaO addition process [21–22]. In addition, this reaction can proceed in air or under inert atmosphere, while enabling the formation of ZnO without carbothermic reduction. In our previous work [21–22], we presented the phase diagram of the $CaO–Fe_2O_3–ZnO$ system at 900 and 1100°C, confirming that, if sufficient CaO is added to $ZnFe_2O_4$, the latter can be transformed into ZnO and $Ca_2Fe_2O_5$ at an equilibrium state beyond the Alkemade line between ZnO and $Ca_2Fe_2O_5$ ($CaO:ZnFe_2O_4 > 2:1$ in moles).

In the present work, we investigated the conversion of $ZnFe_2O_4$ in industrial EAF dust to ZnO in air and in the presence of added CaO; the effect of temperature, reaction time, dust composition, and the amount of CaO added was also examined. Furthermore, the evaporation behavior of the EAF dust components was studied because the preferential evaporation of halides and volatile matters was expected.

2. Experimental

2.1. Materials

Three kinds of EAF dust samples provided by an EAF steelmaking company in Japan were used in this study. Dust A and dust B were collected from conventional EAF operations, whereas dust C was zinc-upgraded dust obtained using dust injection technology, as reported in our previous paper [25]. The chemical compositions of the supplied dusts are shown in Table 1. They were determined by chemical analysis methods explained in section 2.3.

Table 1. Composition of the EAF dust samples supplied by a company that operates an EAF wt%

Sample	Fe	Zn	Mn	Pb	Cd	Cl^-	F^-	$ZnFe_2O_4$	ZnO	$ZnCl_2$
Dust A	31.11	23.60	2.13	1.76	0.01	4.72	1.38	12.55	8.68	2.37
Dust B	26.83	21.56	2.21	1.57	0.02	5.78	0.39	9.26	12.30	0.03
Dust C	21.20	29.64	1.72	1.02	0.02	14.22	0.76	10.00	19.64	0.00

2.2. Experimental procedure

The dust was mixed thoroughly with various amounts of CaO, which was prepared by calcination of $CaCO_3$ (purity > 99.5%, Cica-reagent, Kanto Chemical Co., Inc.) in air at 1100°C for 3 h. 1 g of the dust was mixed thoroughly with CaO in various ratios, and the mixtures were pressed into tablets (outer diameter: 10 mm) under a pressure of approximately 10 MPa. As shown in Fig. 3, each tablet was placed on a platinum sheet in an alumina crucible and heated in a muffle furnace in air for the desired holding time at a temperature ranging from 700 to 1100°C. After being heated, each specimen was quickly withdrawn from the furnace, crushed, and subjected to chemical and X-ray diffraction (XRD) analysis. The reaction degree per unit operation time was determined from the ratio of relative intensities of the XRD peaks of ZnO and $ZnFe_2O_4$ [26–27].

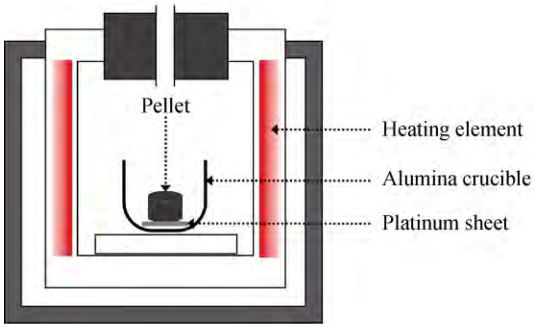

Fig. 3. Schematic of the laboratory-scale furnace.

Dust A was selected for the study of the evaporation behavior of dust components during CaO treatment. Thermogravimetric analysis (TGA) was conducted with a TA Instruments model SDT–Q600 thermogravimetric analyzer to measure the weight change rate of dust A during heating as a function of temperature in the 500–1000°C range. Fig. 4 presents the experimental apparatus used to observe the evaporation behavior of the EAF dust components during heating with CaO under an air stream. Approximately 1-g samples of dust A with and without added CaO were used. Each sample was placed in an alumina combustion boat (width 12 mm × depth 9 mm × length 60 mm) positioned inside a quartz tube reactor (length 33 cm). For the samples of dust A with added CaO, the Ca/Fe molar ratio was 1.3. After the furnace was stabilized at the desired temperature, the quartz tube reactor was fed into the furnace to a given position, and the air flow rate was started at 100 mL/min.

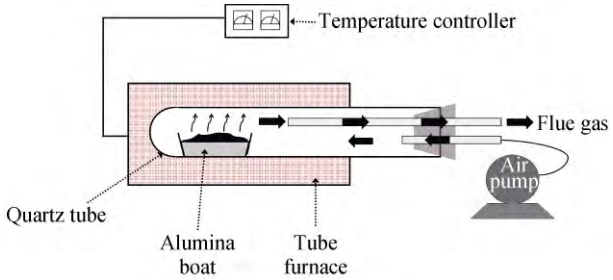

Fig. 4. Experimental apparatus used to observe the evaporation behavior of the EAF dust components during heating with CaO under an air stream.

Each specimen was maintained for 3 h at a temperature that ranged from 550 to 1100°C. After being heated, the specimens were quenched and subjected to XRD and inductively coupled plasma (ICP) analysis.

2.3. Chemical analysis

Wet chemical analysis was conducted to determine the composition of the EAF dust. To determine the total zinc, iron, calcium, manganese, lead, and cadmium contents, a 0.1-g dust sample was fused with 3 g of reagent-grade potassium disulfate ($K_2S_7O_2$) in a platinum crucible, dissolved in HCl solution, and then used for ICP-atomic emission spectroscopy (ICP–AES) measurements on a Shimadzu ICPS–8100. The chlorine and fluorine concentrations were analyzed using pH/ion meters (SevenMulti S80, Mettler Toledo). Generally, EAF dust contains $ZnFe_2O_4$ as the major zinc component, together with some amounts of ZnO and $ZnCl_2$. The chemical species of zinc in the dust were individually determined by the choice of solvent. $ZnFe_2O_4$ is well known to be basically insoluble in either acid or alkaline solution. In the present work, ZnO, $ZnFe_2O_4$, and $ZnCl_2$ in the specimens were individually determined by wet chemical analysis using three solutions; water, the Muspratt solution (a mixture consisting of 10 mL of ammonium acetate, 5 g of ammonium chloride, and 25 mL of distilled water), and fused potassium disulfate. Water can dissolve only $ZnCl_2$, the Muspratt solution can dissolve both ZnO and $ZnCl_2$, and fused potassium disulfate can dissolve all zinc components. By combining the zinc components extracted by these solutions, we determined the amounts of ZnO, $ZnFe_2O_4$, and $ZnCl_2$ in the dust as follows:

$$(\%ZnCl_2) = (\%Zn)_{Water} \times (M_{ZnCl_2}/M_{Zn}) \quad (4)$$

$$(\%ZnO) = [(\%Zn)_{Muspratt} - (\%Zn)_{Water}] \times (M_{ZnO}/M_{Zn}) \quad (5)$$

$$(\%ZnFe_2O_4) = [(\%Zn)_{PD} - (\%Zn)_{Muspratt}] \times (M_{ZnFe_2O_4}/M_{Zn}) \quad (6)$$

Here, $(\%Zn)_{Water}$, $(\%Zn)_{Muspratt}$, and $(\%Zn)_{PD}$ are the amounts of zinc extracted by water, by the Muspratt solution, and by the fused potassium disulfate, respectively, and M denotes the molecular or atomic weight of each species. The principle of this extraction technique was initially confirmed using a mixture of reagent-grade ZnO, $ZnCl_2$, and synthesized $ZnFe_2O_4$.

The structures of the specimens were determined by XRD performed on a Rigaku–RINT2000, together with scanning electron microscopy–energy-dispersive X-ray spectroscopy (SEM–EDX) performed with a JEOL 7500 F–1. XRD patterns of the sample powders were obtained using monochromated Cu K_α radiation; the samples were scanned over the 2θ = 20°–80° range, with a scan step of 0.02° and a fixed counting time of 1 s for each step.

3. Results and discussion

3.1. Characterization of EAF dust

According to Table 1, the major elements in the three dust samples, A, B, and C, were iron and zinc, together with relatively high concentrations of manganese and lead. In addition, these three dust samples contained 4wt%–15wt% of chlorine and 0.4wt%–1.4wt% of fluorine. The iron concentrations in dust A and dust B were comparatively higher than the zinc concentrations, which is a general feature of EAF dust. Conversely, dust C, which was generated by injection technology [25], was enriched with zinc and halogens. As shown in Table 1, $ZnFe_2O_4$ was the major zinc compound in dust A, whereas approximately 40wt% of the zinc existed as ZnO and $ZnCl_2$. ZnO was the major zinc compound in dust B and dust C.

Fig. 5 shows the XRD patterns of the EAF dusts used in the present work. The pattern for dust A indicates that the major components were $ZnFe_2O_4$ and ZnO. The XRD patterns of the three dusts differ slightly, corresponding to the respective ratio of $ZnFe_2O_4$ and ZnO in each dust.

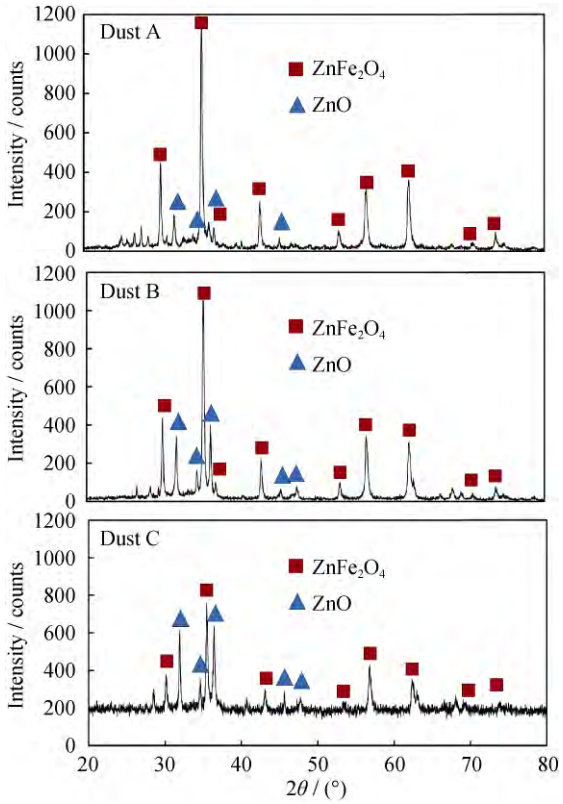

Fig. 5. XRD patterns of the EAF dusts (Cu Kα).

3.2. Conversion rate of $ZnFe_2O_4$ to ZnO in the presence of added CaO

Fig. 6 shows the effect of holding time on the conversion

rate of $ZnFe_2O_4$ in dust A to ZnO and $Ca_2Fe_2O_5$ by means of CaO addition at 1000°C. n_{ZnO} is the moles of zinc oxide, n_{ZF} is the moles of zinc ferrite (ZF), and $n_{ZnO}/(n_{ZnO} + n_{ZF})$ is the relative molar ratio of zinc oxide in total zinc content (zinc oxide + zinc ferrite) indicating conversion rate to zinc oxide. If $n_{ZnO}/(n_{ZnO} + n_{ZF})$ is equal to 1.0, the conversion to zinc oxide is completed. The results indicate that the reaction proceeded quickly and was virtually completed within 1 h, without any change at longer holding times of up to 24 h. At 1000°C, a conversion rate of approximately 80% was achieved for the addition of CaO at a stoichiometric ratio (i.e., 1.0 Ca/Fe). However, the conversion was completed by increasing the amount of added CaO beyond the stoichiometric ratio of Ca/Fe = 1.2. The free energy change in the reaction shown in Eq. (1) exhibited a relatively large negative value of approximately −40 kJ/mol at 700–1100°C [22]; we expect that the reaction shown in Eq. (1) can spontaneously proceed toward right-hand side. The physicochemical nature of this reaction supports the experimental results. Notably, the temperature of the CaO treatment should be less than 1200°C, which is the melting temperature of $Ca_2Fe_2O_5$.

Fig. 7 shows the effect of temperature on the conversion rate of $ZnFe_2O_4$ to ZnO in dust A and dust B when the dusts were heated in air for 1 h. At 700°C, the reaction rate was around 80% at any Ca/Fe molar ratio, indicating that 1 h was insufficient to complete the reaction at this temperature. However, when sufficient CaO was added to bring the Ca/Fe molar ratio to 1.4 and the temperature was in the range of 900–1100°C, the conversion of $ZnFe_2O_4$ to ZnO and the formation of $Ca_2Fe_2O_5$ were almost completed within 1 h for both dusts. This finding indicates that an amount of CaO in excess of the stoichiometric ratio (1.0 Ca/Fe) was necessary to complete the conversion reaction. Notably, the conversion rate decreased at temperatures above 800°C when the Ca/Fe molar ratio was less than 1.4. The XRD patterns obtained under different experimental conditions (Fig. 5) showed that the formation of $ZnFe_2O_4$ from ZnO and the formation of Fe_2O_3 originating from the raw dust were possible when the amount of CaO added was insufficient (Ca/Fe < 1.3):

$$ZnO(s) + Fe_2O_3(s) = ZnFe_2O_4(s) \quad (7)$$

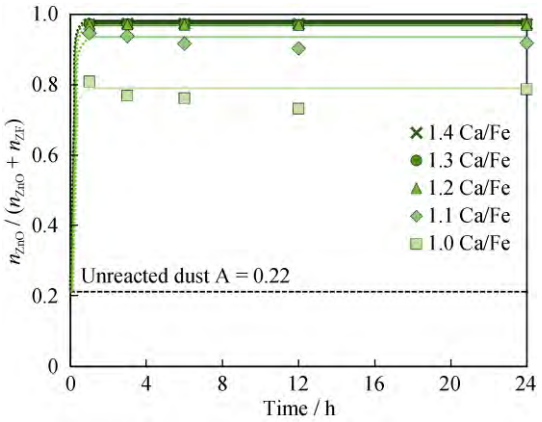

Fig. 6. Reactivity of $ZnFe_2O_4$ in dust A with added CaO at 1000°C as a function of reaction time for different amounts of added CaO.

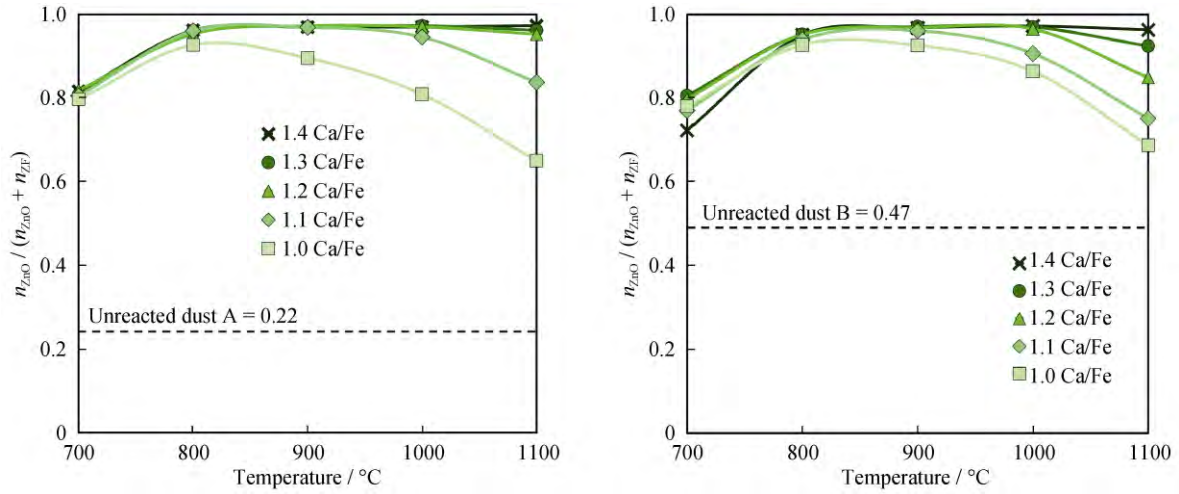

Fig. 7. Reactivity of $ZnFe_2O_4$ with added CaO for 1 h as a function of reaction temperature.

This trend of the formation of additional $ZnFe_2O_4$ became remarkable at higher temperatures and lower Ca/Fe molar ratios, resulting in a lower conversion rate. Fig. 8 shows the relationship between the conversion rate of dusts A, B and C and the Ca/Fe molar ratio when the dusts were heated at 1000°C for 1 h. On the basis of the iron and

$ZnFe_2O_4$ contents in these dusts, the amount of CaO required to complete the conversion was calculated per ton of dust. For example, at 1000°C, the addition of CaO at Ca/Fe = 1.2 was sufficient to complete the conversion for each dust, as shown in Fig. 8, which means that 375, 323, and 255 kg of CaO would be necessary for one ton of dust A, dust B, and dust C, respectively. These results indicate that a lower iron or $ZnFe_2O_4$ concentration resulted in less CaO required for the CaO treatment of EAF dust. Some of the authors have demonstrated that dust recycling to EAF by injection, referred to as the dust injection technology, can increase the zinc content and decrease the iron content in the regenerated dust, indicating that the combination of the dust injection technology and the CaO addition process may reduce the burden for dust treatment [25].

3.3. SEM image and X-ray mapping

The SEM–EDX images of dust A before and after the CaO treatment with 1.3 Ca/Fe at 1100°C for 5 h are presented in Fig. 9. The "as-supplied" EAF dust particles were relatively fine and smaller than 5 μm. Some of the particles were spherical, and EDX revealed that they consisted of zinc and iron, which can be attributed to $ZnFe_2O_4$. However, no $ZnFe_2O_4$ was observed in the EAF dust after the CaO treatment, whereas ZnO and $Ca_2Fe_2O_5$ were observed as 5–10 μm particles in this dust. Therefore, the reaction of $ZnFe_2O_4$ with CaO was confirmed to be completed under these conditions.

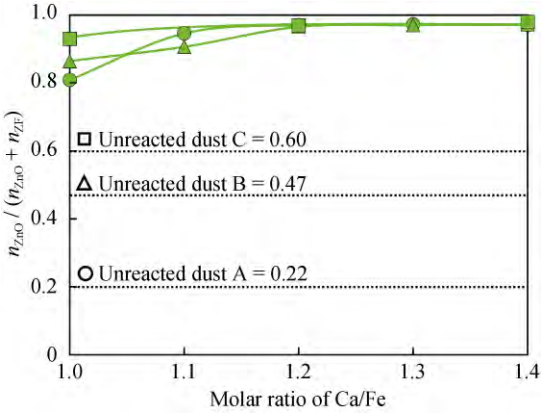

Fig. 8. Reactivity of $ZnFe_2O_4$ with added CaO at 1000°C for 1 h.

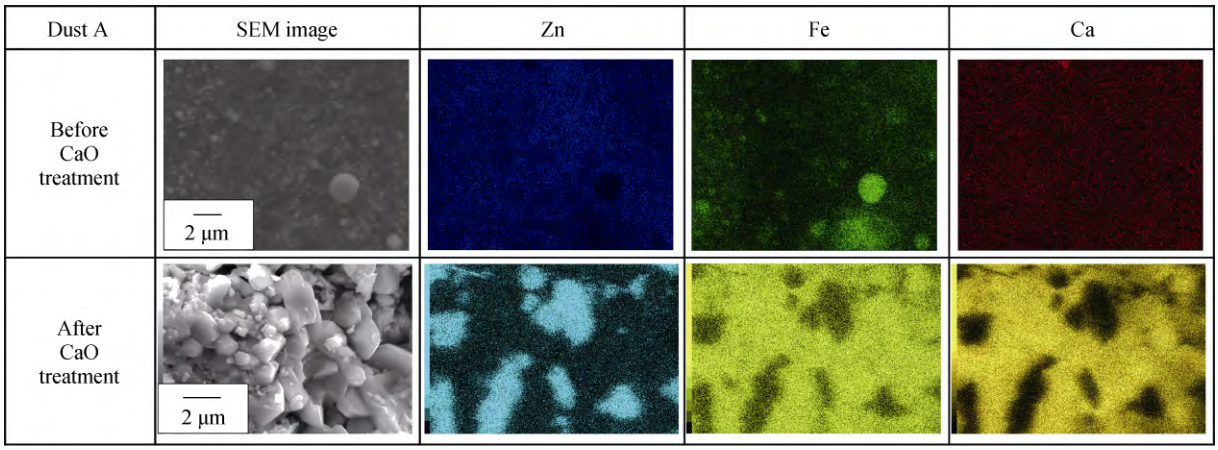

Fig. 9. SEM image and X-ray mapping of dust A before and after CaO addition (1100°C, reaction time = 5 h, Ca/Fe molar ratio = 1.3).

3.4. CaO consumption by other components

Fig. 10 shows the major and minor components (in moles) of the EAF dusts before and after CaO treatment; the amounts of these components were calculated on the basis of the wet chemical analysis results and on the basis of the excess CaO added to the dust. As the figure shows, EAF dust always contains minor minerals such as MnO, MgO, Al_2O_3, halides, etc., and their concentrations vary depending on the operating conditions of the EAF. Most of the halides evaporated during the CaO treatment, as explained in a later section of this paper. However, minor oxides remained in the treated dust; these oxides might have reacted with CaO, resulting in the consumption of CaO prior to its reaction with $ZnFe_2O_4$. This consumption of CaO could be the reason why an excess of CaO was needed to complete the conversion of $ZnFe_2O_4$ to ZnO and $Ca_2Fe_2O_5$. The mechanism of such side-reactions will be investigated in detail in our future work.

3.5. Evaporation behavior of halides and heavy metal

The thermogravimetric analysis of the as-supplied dust A in Fig. 11 showed that dust A exhibited thermal degradation beginning at 660°C and completing at approximately 1000°C,

with approximately 13% total mass loss of the volatiles. After simply heating dust A with and without added CaO, the samples were analyzed by XRD; their XRD patterns are shown in Fig. 12. In the case of simple heating of the as-supplied dust A without added CaO, a significant amount of ZnO, which initially existed in the raw dust, was converted into $ZnFe_2O_4$ via the reaction between ZnO and Fe_2O_3 at high temperatures, as shown in Eq. (7). Meanwhile, ZnO and $Ca_2Fe_2O_5$ dominated the XRD pattern of the dust with added CaO, with no indication of the formation of $ZnFe_2O_4$.

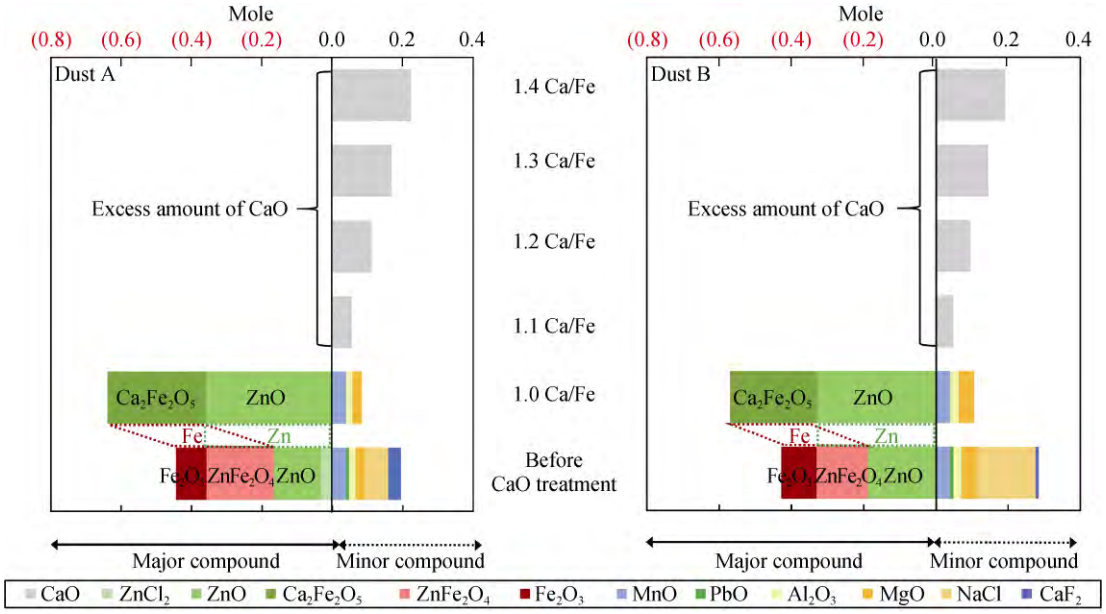

Fig. 10. Mole calculation of components in EAF dust and excess CaO (above the stoichiometric ratio) added during the treatment.

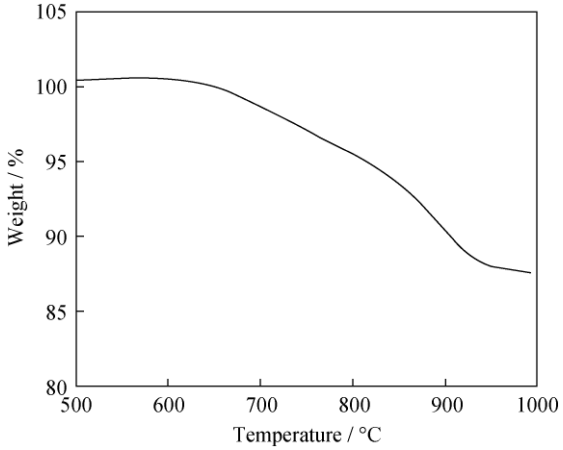

Fig. 11. TGA curve for dust A.

The evaporation behaviors of the components in EAF dust during treatment with and without added CaO were also studied in the present work. The experimental results are presented in Fig. 13 as a function of temperature for 3 h of heating. The evaporation of halogens and lead in the dust without added CaO began at >560°C and drastically increased at ~900°C. Most of the chlorine, fluorine, and lead were preferentially removed from the remaining dust at 1100°C. Similar evaporation behavior of lead and chlorine was observed in the dust with added CaO (1.3 Ca/Fe), whereas the evaporation of fluorine from the dust that was heated with added CaO was slightly shifted toward higher temperatures than that without CaO addition. Most of the lead and chlorine were removed preferentially at temperatures below 900°C, whereas complete removal of fluorine required temperatures above 1000°C. The preferential volatilization of lead, chlorine, and fluorine in the EAF dust is another important benefit of the CaO treatment process. The experimental results of halogen and lead volatilization were in reasonable agreement with the thermodynamic computation results previously published in the literature [13]. Alkaline halides and lead compounds can be vaporized and possibly removed at temperatures as low as 900°C, whereas higher temperatures result in higher vapor pressures of volatile species and oxidizing conditions facilitate the removal of lead in the form of lead oxide. In addition, other researchers have investigated the volatilization reaction of lead and chlorine in EAF dust at reaction temperatures of 700°C to 1000°C in air [17]. Approximately 98% of lead and chlorine were volatized within 90 min at 1000°C. The lead was volatilized as a form of $PbCl_2$ by reacting with NaCl, Al_2O_3, and SiO_2 that were present in the dust; the volatilization reaction was controlled by solid–solid diffusion [17].

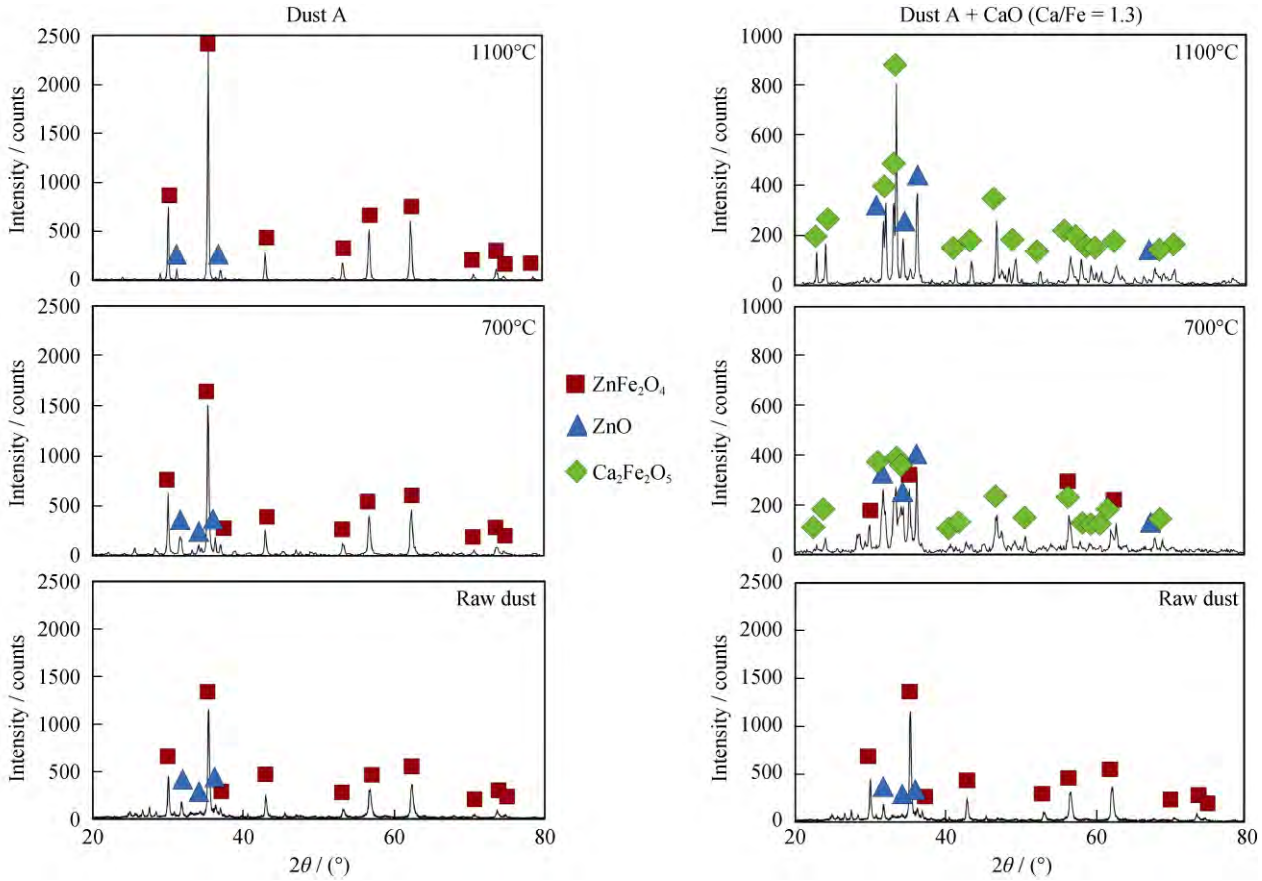

Fig. 12. XRD patterns of dust A as a function of temperature after 3 h of heat treatment with and without CaO addition (Cu Kα).

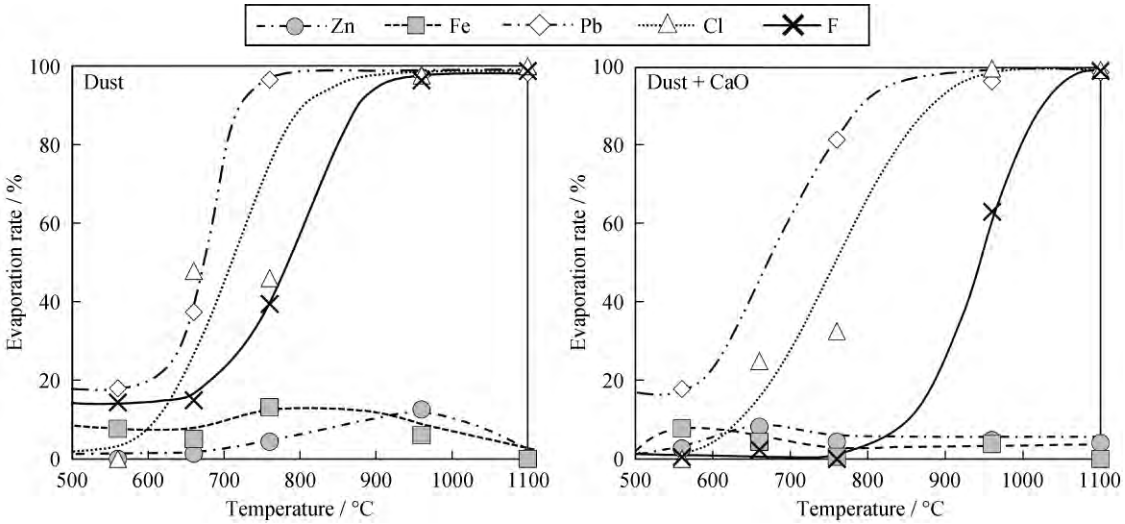

Fig. 13. Evaporation rate of components in dust A as a function of temperature after 3 h of heat treatment with and without CaO addition (Ca/Fe = 1.3).

In the case of the evaporation behavior of iron and zinc, the evaporation losses of zinc and iron from the dust without added CaO were higher than those from the dust with added CaO. According to the low boiling point of $ZnCl_2$ (750°C), $ZnCl_2$ in the dust without added CaO simply evaporates. In contrast, in the case of dust with added CaO, the CaO reduces the amount of $ZnCl_2$ lost by evaporation, as per the following reaction:

$$ZnCl_2 + CaO = ZnO + CaCl_2 \quad (8)$$

The free energy of this reaction is negative at any temperature. Consequently, the added CaO inhibits the evaporation loss of $ZnCl_2$ in the dust to form ZnO in the

CaO-treated dust.

The results of the present work provide us with two important indications: the complete conversion of $ZnFe_2O_4$ to ZnO and the preferential removal of halogens and lead from the dust by the addition of CaO. The former was the beneficial result of the hydrometallurgical treatment of EAF dust because the difficulty associated with leaching $ZnFe_2O_4$, which is the major problem of hydrometallurgical dust treatment, can be avoided. The latter may provide us with the opportunity to produce high-purity zinc metal that is nearly halogen- and lead-free using CaO-treated EAF dust.

4. Conclusions

The conversion of $ZnFe_2O_4$ in industrial EAF dust to ZnO at 700–1100°C in air by the addition of CaO was studied using various amounts of added CaO. Furthermore, the evaporation behavior of the EAF dust components during the CaO treatment process was investigated at various temperatures in air. Specifically, the following conclusions were drawn.

(1) The optimum conditions for the CaO addition process to transform $ZnFe_2O_4$ in EAF dust to ZnO were a processing temperature of 900°C, a processing time of 1 h, and a Ca/Fe molar ratio of 1.1. The $ZnFe_2O_4$ in EAF dust was converted into ZnO and $Ca_2Fe_2O_5$ without carbothermic reduction.

(2) However, to vaporize heavy metals and halogens into the gas phase, the addition of CaO and processing temperatures greater than 1100°C were required. The addition of sufficient CaO to exceed the stoichiometric ratio was also necessary because some CaO was consumed by compounds other than $ZnFe_2O_4$. In addition, lower iron or $ZnFe_2O_4$ concentrations in EAF dust resulted in a lower CaO consumption, especially in the case of dust regenerated from injection technology.

An additional process to separate ZnO and $Ca_2Fe_2O_5$ from the CaO-treated dust is essential. However, this requirement is not as problematic as the separation process required for the as-supplied EAF dust that contains zinc predominantly in the form of $ZnFe_2O_4$. Additionally, the steel industry can use $Ca_2Fe_2O_5$ as a dephosphorization agent or as a raw material for sintering plants. Accordingly, our new process is much more efficient than conventional processes in terms of environmental impact and costs.

Acknowledgements

This project was financially supported by the ISIJ Innovative Program for Advanced Technology, the Iron and Steel Institute of Japan (ISIJ) in 2008–2010. It was supported by a Grant-in-Aid for Challenging Exploratory Research (contract No. 22656171) in 2010–2011 and is supported by a Grant-in-Aid for Scientific Research (Basic Research A, contract No. 25249105) for 2013 through 2015 from the Ministry of Education, Culture, Sports, Science and Technology (MEXT). The cooperation of Aichi Steel Corp. is gratefully acknowledged. We also thank the support provided by the Global COE Program "Materials Integration International Center of Education and Research, Tohoku University", Steel Foundation for Environmental Protection Technology and the valuable comments from members of the division of EAF, ISIJ.

References

[1] R.B. Gordon, T.E. Graedel, M. Bertram, K. Fuse, R. Lifset, H. Rechberger, and S. Spatari, The characterization of technological zinc cycles, *Resour. Conserv. Recycl.*, 39(2003), No. 2, p. 108.

[2] S. Kelebek, S. Yoruk, and B. Davis, Characterization of basic oxygen furnace dust and zinc removal by acid leaching, *Miner. Eng.*, 17(2004), No. 2, p. 285.

[3] N. Leclerc, E. Meux, and J.M. Lecuire, Hydrometallurgical extraction of zinc from zinc ferrites, *Hydrometallurgy*, 70(2003), No. 2, p. 176.

[4] R.A. Shawabkeh, Hydrometallurgical extraction of zinc from Jordanian electric arc furnace dust, *Hydrometallurgy*, 104(2010), No. 2, p. 61.

[5] C.A. Pickles, Thermodynamic analysis of the selective chlorination of electric arc furnace dust, *J. Hazard. Mater.*, 166(2009), No. 2, p. 1030.

[6] A.G. Guézennec, J.C. Huber, F. Patisson, P. Sessiecq, J.P. Birat, and D. Ablitzer, Dust formation in electric arc furnace: birth of the particles, *Powder Technol.*, 157(2005), No. 2, p. 2.

[7] J. Antrekowitsch and H. Antrekowitsch, Hydrometallurgically recovering zinc from electric arc furnace dusts, *JOM*, 53(2001), No. 12, p. 26.

[8] W.J. Bruckard, K.J. Davey, T. Rodopoulos, J.T. Woodcock, and J. Italiano, Water leaching and magnetic separation for decreasing the chloride level and upgrading the zinc content of EAF steelmaking baghouse dusts, *Int. J. Miner. Process.*, 75(2005), No. 1, p. 2.

[9] M. Grabda, S. Oleszek-Kudlak, E. Shibata, and T. Nakamura, Vaporization of zinc during thermal treatment of ZnO with tetrabromobisphenol, *J. Hazard. Mater.*, 187(2011), No. 1, p. 473.

[10] G. Laforest and J. Duchesne, Characterization and leachability of electric arc furnace dust made from remelting of stainless steel, *J. Hazard. Mater.*, 135(2006), No. 1, p. 156.

[11] O. Ruiz, C. Clemente, M. Alonso, and F.J. Alguacil, Recycling of an electric arc furnace flue dust to obtain high grade

ZnO, *J. Hazard. Mater*., 141(2007), No. 1, p. 33.

[12] C.A. Pickles, Thermodynamic analysis of the selective carbothermic reduction of electric arc furnace dust, *J. Hazard. Mater*., 150(2008), No. 2, p. 265.

[13] A. Zabett and W.K. Lu, Thermodynamical computations for removal of alkali halides and lead compounds from electric arc furnace dust, *Calphad*, 32(2008), No. 3, p. 535.

[14] C.C. Wu, F.C. Chang, W.S. Chen, M.S. Tsai, and Y.N. Wang, Reduction behavior of zinc ferrite in EAF-dust recycling with CO gas as a reducing agent, *J. Environ. Manage*., 143(2014), p. 208.

[15] H. Ma, K. Matsubae, K. Nakajima, M.S. Tsai, K.H. Shao, P.C. Chen, C.H. Lee, and T. Nagasaka, Substance flow analysis of zinc cycle and current status of electric arc furnace dust management for zinc recovery in Taiwan, *Resour. Conserv. Recycl*., 56(2011), No. 1, p. 134.

[16] R. Chairaksa, K. Matsubae, K. Nakajima, H. Kubo, and T. Nagasaka, Recovery of metallic zinc from CaO treated EAF dust and its impact on zinc cycle in a nation, [in] *The* 13*th China–Japan Symposium on Science and Technology of Iron and Steel*, Beijing, 2013, p. 215.

[17] J.M. Yoo, B.S. Kim, J.C. Lee, M.S. Kim, and C.W. Nam, Kinetics of the volatilization removal of lead in electric arc furnace dust, *Mater. Trans*., 46(2005), No. 2, p. 323.

[18] C. Peng, F. Zhang, H. Li, and Z. Guo, Removal behavior of Zn, Pb, K and Na from cold bonded briquettes of metallurgical dust in simulated RHF, *ISIJ Int*., 49(2009), No. 12, p. 1874.

[19] T. Havlík, B.V. Souza, A.M. Bernardes, I.A.H. Schneider, and A. Miškufovà, Hydrometallurgical processing of carbon steel EAF dust, *J. Hazard. Mater*., 135(2006), No. 1, p. 311.

[20] G.S. Lee and Y.J. Song, Recycling EAF dust by heat treatment with PVC, *Miner. Eng*., 20(2007), No. 8, p. 739.

[21] R. Chairaksa, Y. Inoue, K. Matsubae, T. Hiraki, and T. Nagasaka, New zinc recovery process from EAF dust by lime addition, [in] *AISTech–Iron and Steel Technology Conference Proceedings*, Pittsburgh, PA, 2010, p. 273.

[22] S. Itoh, A. Tsubone, K. Matsubae, K. Nakajima, and T. Nagasaka, New EAF dust treatment process with the aid of strong magnetic field, *ISIJ Int*., 48(2008), No. 10, p. 1340.

[23] K. Nakajima, K. Matsubae, S. Nakamura, S. Itoh, and T. Nagasaka, Substance flow analysis of zinc associated with iron and steel cycle in Japan and environmental assessment of EAF dust recycling process, *ISIJ Int*., 48(2008), No. 10, p. 1480.

[24] T. Nagasaka, S. Itoh, K. Yokoyama, and K. Nakajima, *Method for Recovering Zinc Oxide from Electric Furnace Dust*, Japanese Patent, Appl. JP5137110, 2013.

[25] A. Tsubone, T. Momiyama, M. Inoue, R. Chairaksa, K. Matsubae, T. Miki, and T. Nagasaka, Dust injection technology for reducing dust treatment burden, *Iron Steel Technol*., 9(2012), No. 7, p. 184.

[26] N. Umeda, *Development on New Treatment Process of Electric Arc Furnace Dust Containing Zinc* [Dissertation], Tohoku University, Sendai, Japan, 2008, p. 34.

[27] Y. Inoue, *Treatment Process of EAF Dust with Lime Addition* [Dissertation], Tohoku University, Sendai, Japan, 2010, p. 42.